A Case Study on Aggregate Load Modeling in Transient Stability Studies

Carlos Grande-Moran
Daniel Feltes
Bernardo Fernandes
James Feltes

Siemens Power Technologies International
Power System Consulting
400 State Street Schenectady, New York 12305

Ming Wu
Robert Wells

ITC Holdings Corp.
ITC Planning
27175 Energy Way Novi, MI 48377

1 Introduction

Replacement of conventional generating resources in power systems with renewable resources, often located far from load centers, and resulting higher power transfers and heavily loaded transmission facilities have brought up many power systems stability issues related to both voltage and frequency. Voltage stability is defined as the ability of a power system to maintain acceptable voltages at all buses in the system under normal operating conditions, and after being subjected to a disturbance from a given initial operating state [1]. Voltage stability issues are related to the lack of sufficient reactive power resources and transmission facilities in locations with a high concentration of industrial, commercial and residential induction motor loads. Instability may occur in the form of a progressive fall of voltage on some buses in a location where there exists a reactive power imbalance between load and generating resources. A possible outcome of voltage instability is the loss of load where the reactive power imbalance occurs or may include the loss of transmission elements or generating plants due to operation of their protective systems, potentially leading to cascading outages. It is important to note that the driving force of voltage instability is generally loads and thus their modeling is of great importance in voltage stability assessments.

Steady state analysis is used as a screening tool to identify those areas in a power system where a reactive power deficiency exists, manifested by the presence of buses where a low voltage magnitude solution is observed. Analysis using simulation of these events using traditional positive sequence dynamics simulation models extends the steady state analysis to show the associated time sequence. However, use of static load models in stability assessment of power system grids masks the influence of motor load on the voltage dip and voltage recovery following a large disturbance. Thus, it is important to model load appropriately in dynamic analysis of power systems to reflect the impact on reactive balance due to the action of induction motor slip adjustment, discharge lighting, power electronics and thermostatically controlled air conditioning, refrigeration and heating loads.

Independent system operators (ISOs) and other operating and planning entities have transient and dynamic stability requirements governing system performance regarding bus voltage dip and voltage recovery following the clearing of a disturbance on the faulted component. These requirements vary among transmission owners and operators with some having tighter thresholds and others having more

moderate ones. However, because of the observed trends of increasing motor and electronic loads in power grids, the use of common values of voltage dip and voltage recovery indices across utility boundaries will help avoid system conditions that may lead to voltage instability. In addition, studies have shown that results from transient and dynamic voltage studies can be significantly impacted by variations in load modeling because of large variations in system voltage where short-term and long-term non-linear load characteristics may play an important role. Considering the stochastic nature of load composition and variation with voltage, it is a challenge to develop practical load models that can be used in power system planning and operation studies concerned with delayed voltage recovery.

2 Fault Induced Delayed Voltage Recovery (FIDVR)

The North American Electric Reliability Corporation (NERC) defined FIDVR [2] as a voltage condition initiated by a fault and characterized by:

- Stalling of induction motors
- Initial voltage recovery after the clearing of a fault to less than 90 percent of pre-contingency voltage
- Slow voltage recovery of more than two seconds to expected post-contingency steady-state voltage levels

FIDVR phenomena is caused or aggravated by large amounts of induction motor loads; in particular single phase air conditioner load. This type of load plays a main role in FIDVR events because of its low inertia and hence its predisposition to stall. Once a single-phase air-conditioner compressor stalls, it will draw currents that are in the range of four to six times its nominal value, making it more difficult for the power system and its reactive power resources to be able to recover the voltages to acceptable levels in post-disturbance conditions. The technical literature sometimes refers to FIDVR events as a "wide-area high impedance distributed fault". Figure 1 shows typical FIDVR event characteristics. [3]

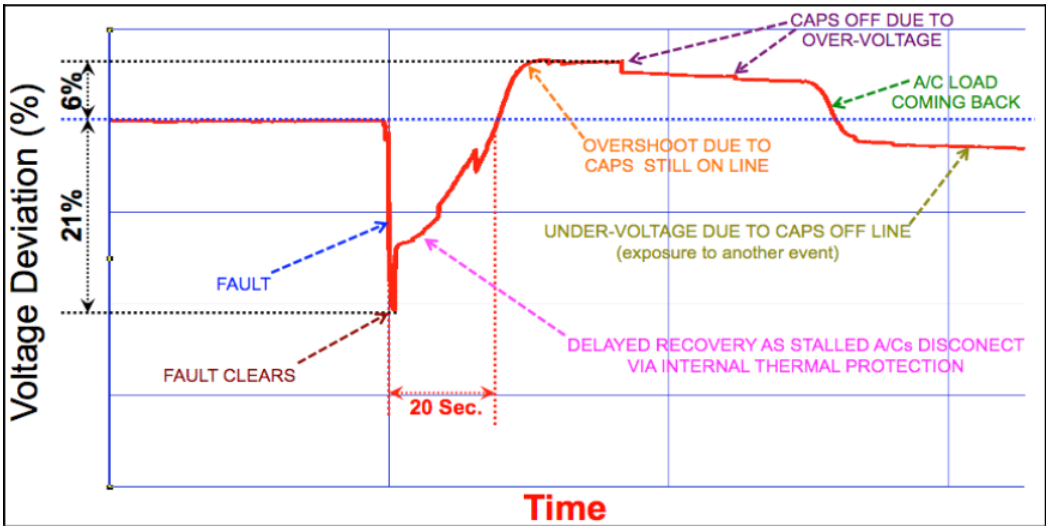

Figure 1. Typical FIDVR Event [3]

When FIDVR events affect the bulk power system, the situation becomes one of elevated risk, as it can trigger further losses of load and generation and even cascading events potentially leading to a blackout. Therefore, accurate load modeling is a requirement to study FIDVR events.

Traditional system studies have not been able to replicate measured FIDVR events accurately due to the use of load models that are not able to accurately represent the loads and its dynamics. Voltage dependent static load models work well for system studies when the load composition does not have a high penetration of single-phase induction motors. However, FIDVR event analysis requires dynamic simulations utilizing load simulation models that appropriately represent a much more wide variety of load dynamics.

3 Voltage Criteria

Industry research indicates that it is not possible to avoid FIDVR events given the very short time required to stall compressor driven motors, such as single phase air conditioners [4]. This type of load can stall during faults cleared as fast as 3 cycles if the voltage at the motor terminals drops below 60% to 70%, depending on the A/C unit and the outdoor temperature. The stall voltage is relatively constant as the duration of the voltage sag is varied from 3 cycles to 30 seconds.

The objectives of a dynamic voltage criterion are to ensure the fault ride-through by the generators and the majority of the loads, and to minimize the risk of additional motor stalling, generator tripping or voltage collapse.

Load lost as a result of a disturbance can be divided into two categories:

a) Consequential load loss – load no longer served as a result of transmission facilities being removed from service to isolate the fault, as well as loss of voltage sensitive load due to the voltage dip caused by the fault

b) Non-consequential load loss – loss of additional load due to FIDVR.

Motor stalling due to the initial voltage dip caused by the fault is unavoidable, but the criteria should minimize the risk of additional motor stalling.

Air conditioner tests performed by the Lawrence Berkley National Laboratory [4] indicate that compressor motors that do not stall as a result of the fault will not stall as long as the voltage at the terminals of the air conditioner remains above the stall voltage. However, one can question whether or not the minimum voltage level specified in most of utilities' voltage criteria will keep the air conditioner terminal voltage above the 60% to70% stall voltage when the air conditioner will draw 150% to 200% of rated current at 70% rated voltage.

Most ISOs, Reliability Coordinators (RCO) and utilities use similar transient voltage recovery criteria, consistent with the NERC reliability guidelines [5]. An example of typical voltage recovery criteria is shown in Table 1.

Table 1. Typical Voltage Recovery Criteria Adopted by Utilities, ISOs and RCOs

Planning Events P1-P2		Planning Events P3-P7	
Load Bus Voltage Must Recover To (pu)	At or Before Time (sec after fault clearing)	Load Bus Voltage Must Recover To (pu)	At or Before Time (sec after fault clearing)
0.8	2.0	0.8	4.0
0.9	10.0	0.9	10.0

With respect to the risk of generator tripping, the purpose of the proposed NERC Standard PRC-024-1 [6] is to ensure generating units remain connected during voltage excursions. The utilities' and ISO's criteria should be consistent with PRC-024 Attachment 2 (see Figure 2). The standard has exceptions for existing units where equipment limitations prevent compliance, but generator owners are required to provide an estimate of unit performance during voltage excursions so the risk of units tripping can be further evaluated. Voltage at generating stations will generally be higher than at load buses, which mitigates to some degree the risk of generators tripping.

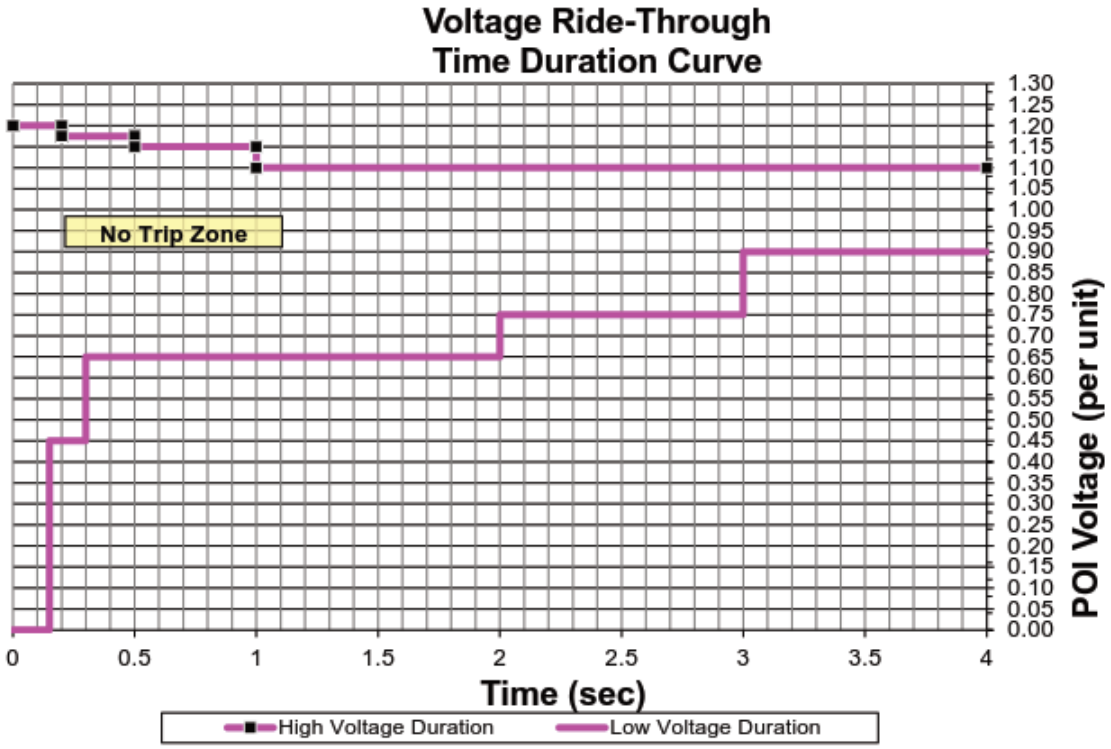

Figure 2. NERC Standard PRC-024 Attachment 2

4 Historical Load Models

A closer look into the response and dynamic performance of controllers used in the control of conventional and renewable generating resources' terminal voltage and voltage at the point of

interconnection of generating plants is an important task for analysts to carry out prior to dynamic simulation of critical events that adversely impact voltage in the post-contingency state of a power system. This task may reveal the presence of slow response or poorly tuned controllers that may impact the response from generating sources to balance the reactive power demand from dynamic (motors) and static (ZIP type) loads in the system. Shunt reactive power compensating devices (SVC, STATCOM, fixed and mechanically switched capacitors and reactors) controllers' time response and performance need to be checked as well. It is important to note that this check is most critical for reactive power resources electrically close to the area where low voltage issues are observed in the steady state analysis.

Since loads are a main driving force in the dynamic response of power grids subjected to large variations in system voltage in this type of study, it is important that the system models include accurate representation of these loads with respect to both voltage and time. These effects include the inertial and machine flux dynamics of induction motor loads as well as the dynamic response of motor protection systems (thermal and undervoltage) and also the sensitivity of static and electronic loads to voltage and frequency variations. These are aggregated models that combine the effects of loads, shunt compensating devices, feeders and transformer voltage regulators "downstream" of a distribution substation. These simplified equivalent models thus will represent the dynamic performance of the aggregate of all "downstream" loads, controls and distribution system components.

The number and type of loads connected to the system changes continuously with time. Consequently, the magnitude, composition and dynamic response of the load may change with season, month, week, day and hour of the day. This unpredictable and somewhat random behavior of the system load makes its modeling difficult in power system studies.

Historically, static load models responsive to voltage variations were used in the assessment of voltage recovery in power grids. These algebraic characteristic load models may include a component that is independent of voltage (constant MVA – P component), a component that varies linearly with voltage (constant current – I component) and a component that varies with the square of the voltage (Constant impedance – Z component). Linear combinations of these three types of static load models are known as ZIP models. A combination of 100% constant I for active power load and 100% constant Z for reactive power load has often been used in dynamic simulations if no additional information is available. However, in system wide studies, each control area generally had its own combination of ZIP load model components.

If load dynamics, that is variation with time, are to be included in load models then power system analysts have a choice of composite or complex load models and induction motor load models. The simplest complex load model (CLOD) [7] consists of two types of three-phase induction motor load (small and large double cage types), discharge lighting load, saturation of distribution transformers, and static load consisting of a constant MVA component and a second load whose active power component varies with a specified exponent Kp and reactive power components varies with voltage squared (constant Z). Each of these load components are specified as a percentage of the total aggregated bus load. The induction motor components model the inertial dynamics and motor steady state electrical characteristics. The discharge lighting component is modeled as constant I for its active power component and its reactive power component varies with voltage raised to the power 4.5. In addition, the discharge lighting component is turned off whenever the bus voltage is below 0.65 per unit and reduced linearly if the bus

voltage is between 0.75 per unit and 0.65 per unit. The saturation effect of distribution transformers can be modeled but should not exceed 10% of the total bus load current in the model. The load model is connected to the power system model bus by way of a transformer with taps on the primary winding and impedance R +j X in per unit on the MW bus load base for modeling the transformer leakage impedance and distribution feeders. At the initialization of the dynamic model, an off-nominal tap is calculated for the transformer so that the voltage magnitude of the internal bus where the load is connected is 0.98 per unit. The apparent power rating of the induction motors is calculated from the percentage specified for each of these motors. The inertia constants (motor rotor + mechanical load) are assumed by the model as H = 1.0 kW-s/kVA for the large motor component and H = 0.6 kW-s/kVA for the small motor component. A rule of thumb to use for the percentage of large and small 3-phase induction motor load is that motor with nameplate rating of 200 HP and above will be considered large, and ratings below 200 HP will be considered small. Note that there no is voltage, frequency or thermal protection represented in the model. Figure 3 shows a graphical representation of this model.

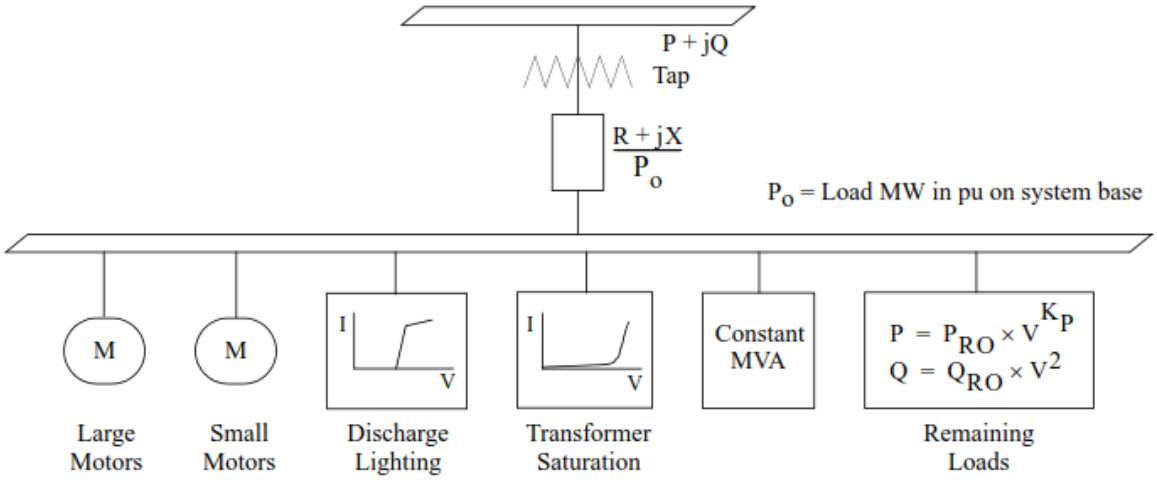

Figure 3. Complex Load Model (CLOD)

The use of this model is recommended for initial screenings to identify voltage performance issues following the removal of the fault and/or faulted element(s) in the grid. Its simplicity makes it easy to use in power system studies since the inputs to the model are just the percentage of the total bus load allocated to each load component. However, if the study area of the system considered for analysis includes large amounts of residential heating, refrigeration and air conditioning load that use single phase induction motors, these loads cannot be fully modeled in the complex load model. Thus, to include the 3-phase induction motor flux, single phase induction motor load and frequency variation dynamic effects a more detailed model is required.

A composite load model (CMLD) that includes the dynamics missing in the complex load model described above is available [8]. Figure 4 shows a graphical representation of this model.

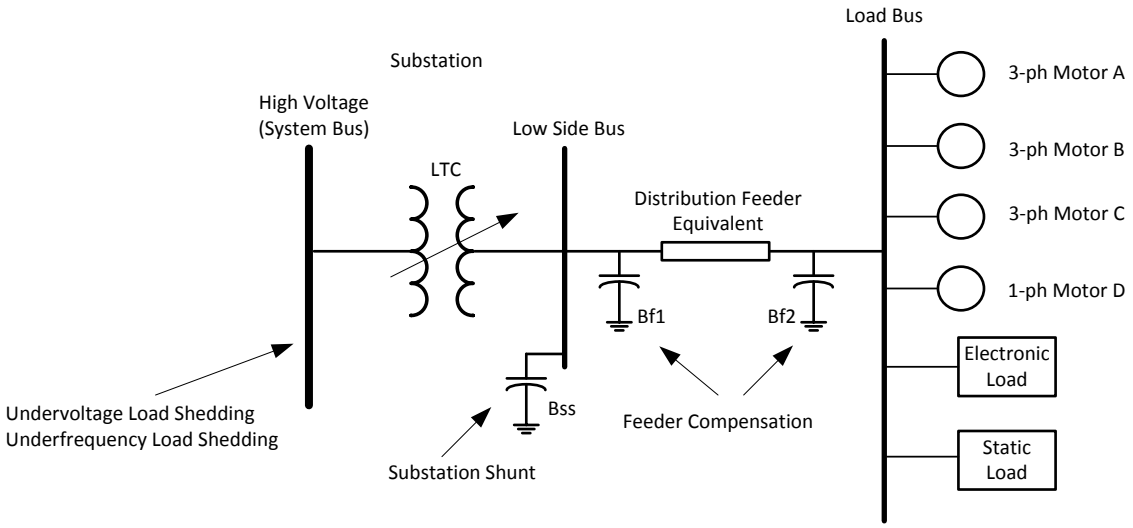

Figure 4. Composite Load Model (CMLD)

The composite load model includes the following components:

1. A 3-phase induction motor type A. This type represents small and large motors used in commercial cooling and refrigeration and central cooling systems used in large commercial buildings. Typical ratings for the small motors are between 5 to 15 HP and for large motors are 200 to 500 HP. This type of motor has a high starting torque and typically drives a constant torque load. It has an estimated average total inertia (motor + load) of 0.1 kW-s/kVA and includes undervoltage protection.
2. A 3-phase induction motor type B. This type represents small induction motors used with ventilation and air-handlers fans in residential and commercial buildings. Typical rating is 5 to 25 HP. Load torque is proportional to speed squared and inertia constants are in the range of 0.25 to 1.0 kW-s/kVA. It represents a NEMA type B motor design and includes undervoltage protection.
3. A 3-phase induction motor type C. This type represents small induction motors used with water circulating pumps in central cooling systems. Typical rating is 5 to 25 HP. Load torque is proportional to speed squared and inertia constants are small, in the range of 0.1 to 0.2 kW-s/kVA. It represents a NEMA type B motor design and includes undervoltage protection
4. A single phase induction motor type D. This type represents small motors used with compressors in residential and small commercial cooling and refrigeration. Typical rating is between 3 to 5 HP. A constant torque load characteristics and very small inertia makes these motors prone to stall. They also can have quick restart. This motor type includes thermal overload, magnetic contactor and undervoltage protection.
5. An electronic load component. This model is defined by 4 parameters: power factor, voltage at which the load starts tripping, voltage at which all load is tripped and voltage at which the load will automatically reconnect. The tripping of electronic load varies linearly with voltage between the two load tripping voltage thresholds. This load is considered a constant power load until the voltage drops to the voltage at which load starts tripping.

6. A static load component sensitive to voltage and frequency variations. This model is defined by 6 parameters: power factor, two exponents for active power components sensitive to voltage variation, two exponents for reactive power components sensitive to voltage variation, and a factor to include the sensitivity of the static load to frequency variation. The model also includes a constant power component which is calculated as the load fraction remaining after assigning the load fractions components associated with the exponent. The equation for the power variation is shown below (the expression for reactive power has the same form).

$$P = Po * (P1c * (V/Vo)^{P1e} + P2c * (V/Vo)^{P2e} + P3) * (1 + Pfrq * \Delta f)$$

7. A substation transformer model. The transformer model includes the transformer's leakage reactance in per unit on load MVA base, a fixed tap on the HV winding set to nominal (1.0 pu) and an adjustable tap on the LV winding. The default number of taps is 33 with a tap range of ±10%, which leads to a step size of 0.00625 pu. The LV transformer terminal voltage is controlled by the tap. The default voltage control band for the controlled bus voltage is 0.9875 pu to 1.0125. If tap adjustment is used in dynamic simulations, two parameters should be specified: the LTC time delay to initiate tap adjustment and the LTC time delay between tap adjustments.
8. A main feeder model connecting the substation transformer to the bus where the aggregated load model is connected. The model includes the feeder series impedance in per unit on load MVA base, shunt compensation at the LV bus of the transformer substation and feeder compensation at the its sending and receiving ends.
9. Load Shedding for underfrequency and undervoltage. The model is responsive to UFLS and UVLS relays associated with the HV bus (network bus) of the transformer substation. The fractions of the composite load that will be shed are based on the number of steps and thresholds specified with the UFLS and UVLS relays. The transformer tap setting and the substation shunt compensation in the model remain the same after any relay action.

The CMLD requires specifying the fractions of the total load specified in the load flow model associated with motor load type A, B, C and D and the electronic load. The fraction associated with the static load is what remains after adding up all fractions associated with the motor and electronic loads. These fractions are dependent on the load composition at each load bus in the power system model. When no distribution substation data is available, many utilities use zonal or regional seasonal data that is available from some independent system operators [9,10].

When industrial loads with large induction motors are present in the study area, it is recommended to use a dynamic model that includes both inertial and machine flux dynamics in transient and dynamic voltage studies. The data needed for the modeling of very large induction motors are the motor circuit parameters, R's and X's (or the associated time constants and reactances), associated with the stator and rotor windings and the excitation current requirements (magnetization reactance) used in the equivalent circuit model that includes these R's and X's, the running slip (the relative speed between the rotor and the rotating field in the motor's air-gap travelling at synchronous speed), the total inertia of the motor's rotor and the mechanically driven load, and speed characteristic of the load torque – for example, constant, proportional to speed, or proportional to speed squared. If these parameters are not available from the motor's manufacturer, estimation of the circuit parameters can be obtained from the knowledge of the motor output torque, motor current and power factor at starting, maximum torque and running

operating point (defined by the interception of the torque-speed characteristics of the motor and mechanical load.). In addition, the motor efficiency at rated load is needed to calculate the motor kVA rating along with the nameplate output HP and the operating power factor at rated load. If the full-load line current is known, the three phase motor kVA is calculated from √3*Irated*Vph. Figure 5 shows the graphical representation of this model. Note that the model represents a double squirrel cage model which is the design generally found in large induction motors. A very large reactance in the second branch of the model can be used to represent a single cage motor.

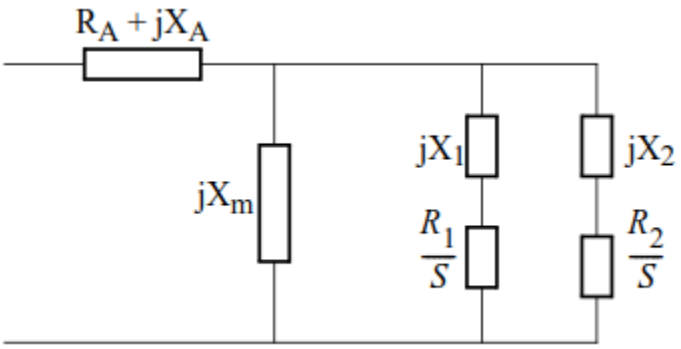

Figure 5. Induction Motor Equivalent Circuit Model

Note that all of these dynamic load models are represented as static loads in the load flow model. Since step-down transformer taps, distribution voltage regulators and shunt compensation keep the voltage profile in distribution systems fairly constant, a constant power or MVA representation is recommended for representation in the load flow model of the power system.

5 Case Study

A case study is presented in this section to show the methodology used when performing transient voltage response studies. The main objective of the study is to assess the dynamic performance of the system regarding voltage recovery following the clearing of the event causing a large voltage variation in the study area. This assessment is used to verify whether a transmission operator is in compliance with the NERC Standard TPL-001-4 R5 [11] and, in the event of finding any violations to this standard, identify the proper corrective action plan to mitigate or eliminate, if possible, these violations.

Each Transmission Planner and Planning Coordinator is responsible to have a transient voltage response criterion that at a minimum specify the voltage level and maximum length of time that transmission system voltages can be below immediately after clearing a system fault (voltage dip) and a few seconds after removing the fault (voltage recovery.) Typical level and length of time selected for the voltage dip criteria are 70% and 5 cycles after the fault clearing, respectively. Typical level and length of time for the voltage recovery are 80% to 93% and 1 to 15 seconds. Note that there is a direct relationship between the selected criteria and the required reactive reserves. Strict requirements will mean that significant reactive power reserves will need to be in place to support the system voltage transient response. Transient voltage response studies are important in assessing and quantifying the reactive power resources available to have an adequate transient voltage response.

The transient voltage response criteria used in the case study is:

1. Bus voltages shall not dip below 70% of the nominal voltage for more than 83.3 ms (5 cycles) after fault clearing.

2. Bus voltages shall recover to the acceptable steady state low voltage limit within 5 seconds after fault clearing. The steady state low voltage limit is 0.93 pu for all buses100 kV and above.

The study area used in the case study included all of the transmission voltage levels above 100 kV, including operating voltages of 115 kV, 138 kV, 161 kV and 345 kV. The study area has a total on-line generation of 4,200 MW, serving an estimated total load of 4331 MW (peak 2017 values). The system includes fixed and mechanically switched reactive compensation. The main load center is served from two major power plants, one of which is a nuclear generating facility operated as a base load plant. The total generation from these two plants is about 900 MW. The nuclear power plant generating unit is the largest source of reactive power capability in the area.

A high percentage of the load served in the study area is made up of three phase induction motors (industrial and commercial loads), single phase induction motors (residential and small commercial loads) and electronic devices (commercial and residential loads). Under normal operating conditions, system voltages are close to their nominal value with some buses slightly higher or lower, up to 3% above and 1% below their nominal value.

The breakdown of the control area native load by class is provided in Table 2.

Table 2. Study Area Aggregated Load Composition by Load Class

Zones	A (%)	B (%)	C (%)	D (%)	E (%)	F (%)
Industrial	11	0	46	19	21	40
Commercial	51	67	28	17	44	25
Residential	38	33	26	64	35	35
Agriculture	0	0	0	0	0	0

The composite load model (CMLD) described above was used in the transient voltage response study. The percentages by load class in Table 1 are converted into the six components of the CMLD using expressions provided by the System Operator of the grid [10] The following percentages of each of the six components by zones is shown in Table 3.

Table 3. Percentage of Aggregated Composite Load Components by Zone

Load Type	A (%)	B (%)	C (%)	D (%)	E (%)	F (%)
Motor A	11	11	11	10	11	11
Motor B	10	9	15	10	11	14
Motor C	5	3	9	5	6	8
Motor D	26	28	16	26	23	18
Electronic Load	18	17	21	18	19	21
Static	31	32	28	31	30	28

The study of transient and dynamic system voltage response needs to look at the worst credible system conditions. Thus, such studies generally start from a heavy loaded operating condition where generating resources are operating close to their reactive power capability limits. This can lead to a system voltage profile in some areas of the power system with bus voltages close to the normal operating lower limit and in some instances even slightly below it. If the power system has a significant penetration of renewable resources, then a condition where conventional generation is replaced with renewable resources can also be used to create a "stressed" case. The proper selection of the base case load flows, particularly with respect to the generation dispatch, load level and area imports, to model severe but representative initial conditions is an important first step. These steady state solutions will be used to initialize the dynamic components in the stability assessment of the power system.

In this study, transient voltage response was assessed using three operating scenarios. Two represented present conditions. The first modeled summer peak load with wind resources dispatched at 20%. The second case also modeled summer peak load but with wind resources dispatched at 67% output (i.e., the "heavy wind case"). The third case represented the planning horizon, 2026 in this case, also modeled summer peak load conditions with a wind resources dispatched at 20%. For each of these three operating scenarios, two generation dispatches were considered, one called a "normal" generation dispatch with typical conventional generation on line and a second dispatch called the "stressed" generation dispatch where 895 MW of conventional generation (about 20% of the area total) was turned off in the study area and replaced by scaling down load in the neighboring control areas, maintaining a constant P/Q ratio. The purpose of the second case is to reduce the reactive power resources in the study area to assess the impact of the high penetration of renewable resources on transient voltage response requirements.

A total of 80 fault cases that may cause critical voltage scenarios in the study area were tried. The type of system faults tested in each of the six operating scenarios included:

1. Bolted three-phase faults cleared by primary relay system action (TPL P1 type)
2. Bolted three-phase faults with one system component out of service (generator, transmission line, power transformer, breaker or protection relay system) prior to fault inception (TPL P3 and P6 type)
3. Bolted single-phase to ground faults resulting in delayed fault clearing due to breaker failure and subsequent inadvertent breaker failure event outages (TPL P4 type)
4. Bolted single-phase to ground faults at a circuit breaker (TPL P2 type)
5. Bolted single-phase to ground faults with delayed clearing due to single point of failure (SPOF) event on relay protection systems (TPL P5 type)

Aggregated load models based on the composite load model CMLD were implemented in each of the 6 zones of the study area and included in the study area dynamic data base. Investigations were performed to determine the appropriate load model parameters. Two sets of parameters for the composite load model (CMLD) were used as starting point for this sensitivity analyses. The first was a set proposed by the Electric Power Research Institute (EPRI) [12] and a second set proposed by the Western Electric Coordinating Council (WECC) [13]. Both sets are included in Appendix A of this paper. The results from these analyses was used to identify the composite load model parameter set that provided results that were in line with historical voltage events observed in the study area. This final parameter set is also included in Appendix A.

It is illustrative to show some simulations results that demonstrate the basic phenomena. The initial dynamic simulations were performed using the CMLD load model with the undervoltage protection system associated with the motor load disabled. These simulations caused a significant amount of voltage violations. Due to the voltage depression during the fault, the motors near the fault will stall and draw more reactive power. If the trip settings are disabled, then these motors will remained stalled and the associated higher reactive power draw will continue to bring the voltage down. When the trip settings are enabled, the tripping of the motors reduces the associated reactive power requirements and the voltage recovery is much faster. Figure 6 shows a comparison of the simulation of a stuck breaker fault on the 161 kV system with three variations of the load model: without the CMLD model (black curve), using the CMLD model without tripping (blue curve) and using the CMLD model with tripping (red curve). Note that without the CMLD model, that is, with a ZIP load model, the voltage recovery is instantaneous and voltage recovers to near normal conditions immediately following the clearing of the fault (it is a bit lower due to the transmission outages associated with the fault). Without motor tripping, the voltage following fault clearing is about 0.8 pu and rises to about 0.91 pu over the 0.5 seconds. With motor tripping, the voltage following fault clearing is about 0.89 pu and the post fault voltage dip is smaller.

Figure 7 shows the motor A component active and reactive power at the same bus as in Figure 6, both with and without modeling of the motor protection. Motor A represents small and large three phase motors used in commercial cooling and refrigeration. These motors have a low inertia, 0.1 pu in these simulations. The motor A component active power and reactive power without the tripping logic active are shown by the black and blue curves respectively, while the active power and reactive power with the tripping logic active are shown by the red and pink curves respectively. The low voltages during the fault and following the fault clearing cause a drop in motor active power, causing the motors to slow and draw more reactive power. Motor tripping due to the undervoltage protection is seen by the drop in power (red curve) at about 1.1 seconds. Note that some of the motors that are tripped will be able to restart. The restarting is seen at about 1.4 seconds. Restarting of the motors will cause a high demand for reactive power leading to a drop in voltage at this time, as can be seen in Figure 6. Of course, the bus voltage magnitude is influenced by the response of all of the load components, not just the motor A component shown in Figure 7.

Figure 8 shows the same voltages plotted earlier in Figure 6, but this time with an expanded time scale of 15 seconds to show the long term recovery. Without the modeling of the motor protection action (blue curve), that is no motor tripping, the motors remained stalled and voltages do not recover to normal levels. The voltage with motor protection active (red curve), that is with motor tripping, shows the voltage recovering to normal over about a 7 second period. This slower recovery in voltage is related to the tripping of the non-recloseable part of motor D (single phase air conditioner motors). These motors trip due to the motor D thermal relay in response to the increase in motor temperature resulting from the higher stall current. The tripping is modeled as occurring over a period of time, approximating that the represented air conditioners have somewhat different tripping characteristics. This tripping starts at about 4.3 seconds and all of these motors have been tripped by 11.5 seconds. One can see that the period of the tripping of these motors coincides with the rise in voltage seen in Figure 8. This is due to the reduction in the real and reactive power drawn by these stalled motors.

The motor speeds for the motor A (black curve), motor B (blue curve) and motor C (red curve) components are shown in Figure 9. Note the much larger speed deviation in motor A due to its low inertia

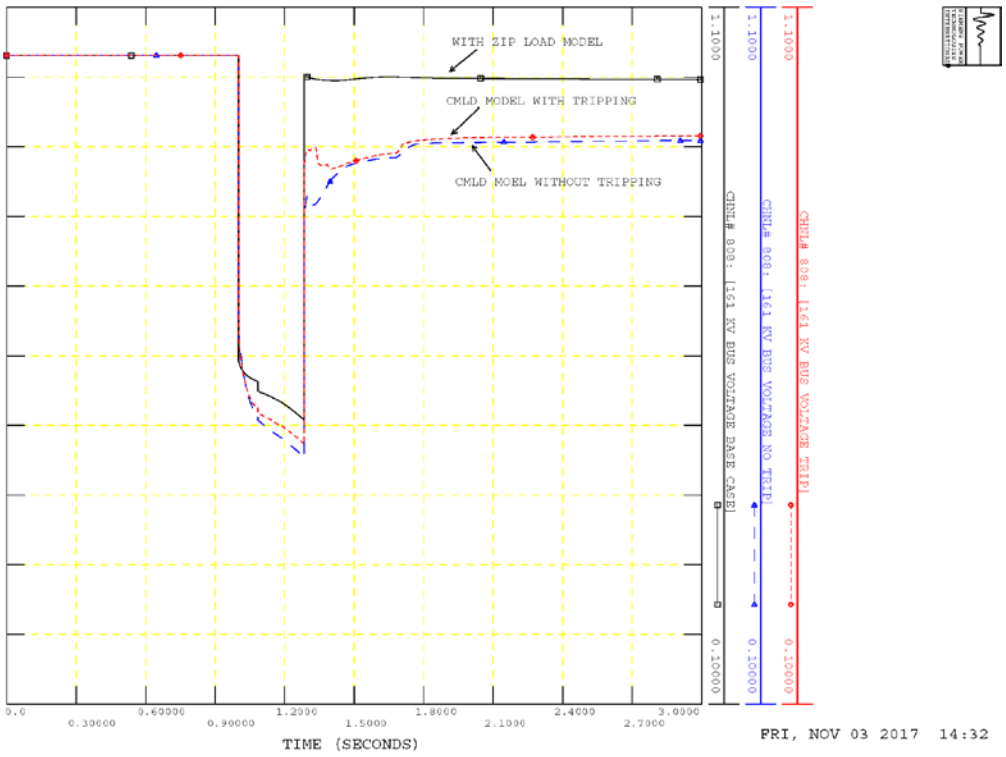

Figure 6. Plot of 161 kV voltage for stuck breaker fault with three variations of the load model: without the CMLD model (black curve), using the CMLD model without tripping (blue curve) and using the CMLD model with tripping (red curve).

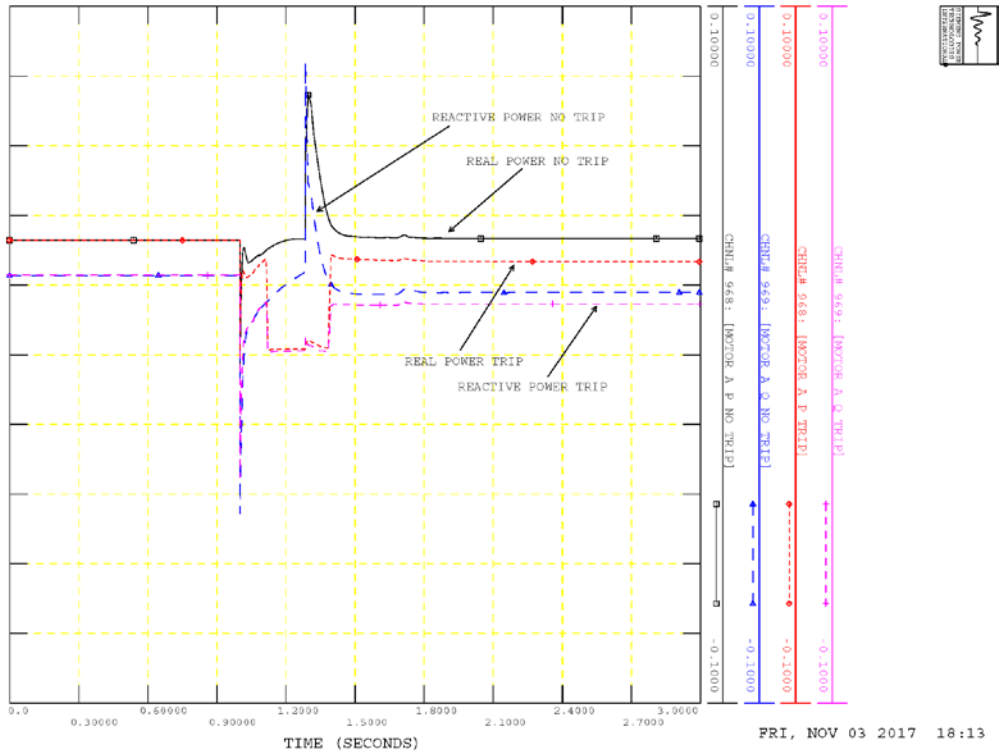

Figure 7. Plot of motor A component active and reactive power for stuck breaker fault.

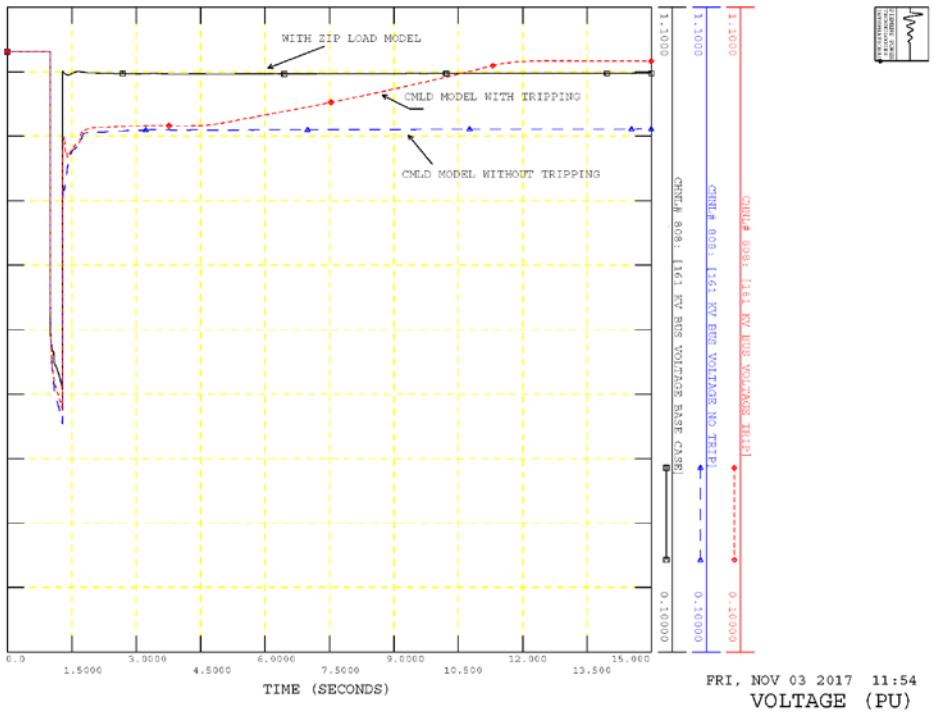

Figure 8. Plot of 161 kV voltage for stuck breaker fault with three variations of the load model

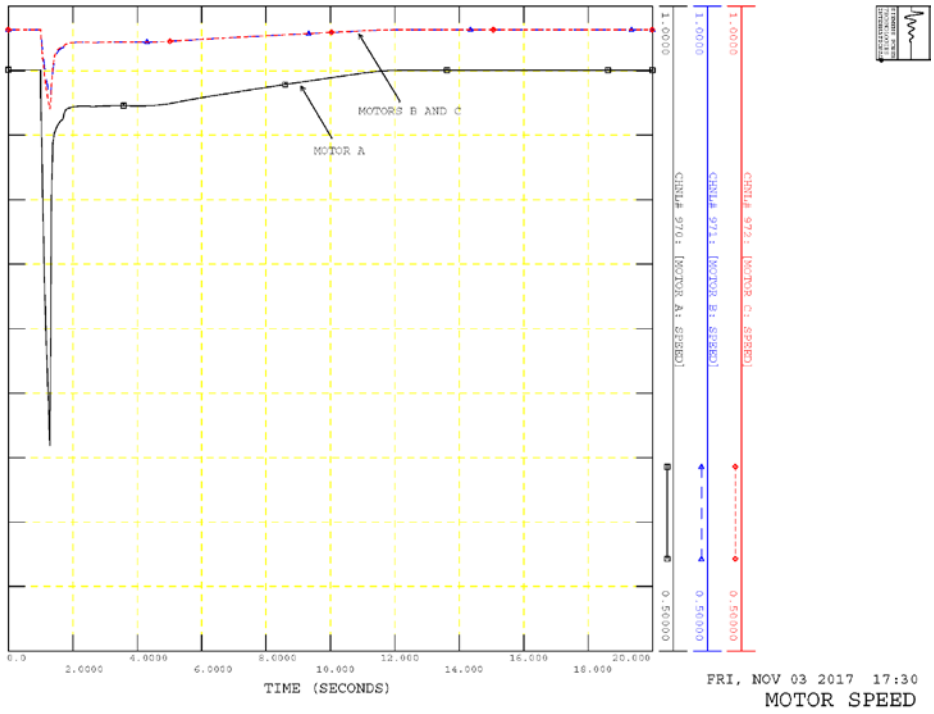

Figure 9. Plot of motor speed for motor A (black curve), motor B (blue curve) and motor C (red curve) components

and constant torque load characteristic. The motors all recover to operating speed shortly after fault clearing. One can also see the effect of the rise in voltage on the speeds of these three phase motors. As the voltage rises, the slips of these machines decrease due to the effect of voltage on the torque-slip characteristics of the motors.

The voltage in Figure 8 with the motor tripping rises above the voltage using the ZIP load model as some of the motors (for example, about 20% of motor A) do not reclose. This can also be seen in the active power of the motor A component in Figure 7.

These simulations were used to identify the system fault events and operating scenarios causing the worst voltage violations. The summer peak operating scenario with high wind turbine generating units dispatched at 20% did not cause severe voltage violations in the study area because of a significant amount of reactive resources available in the on-line conventional generation. The future year summer peak scenario also did not cause severe voltage violations in the study area due to the available reactive resources and because of a large number of transmission upgrades being put on line in this future planning scenario. However the summer peak operating scenario with wind turbine generating units dispatched at 67% showed the most low voltage concerns and was selected for further analysis. Out of all the fault events tested, five faults were found to be the most critical ones. Using this scenario and these critical system faults, a sensitivity analysis was performed to determine the appropriate parameter set for the undervoltage protection system associated with the three-phase and single phase induction motor components of the composite load model CMLD.

Dynamic simulations performed with the final parameter set for the composite load model in the study area were then used to identify locations in the study area where the transient voltage response requirements of the transmission operator were violated when applying the critical system faults. It was found that the 161 kV transmission network in the vicinity of the nuclear power plant showed a post-contingency operating state that is deficient in reactive power, leading to delayed voltage recovery with a post-contingency voltage profile below the required threshold five seconds after fault clearing. It is important to note that slow voltage recovery and noncompliance with the voltage response threshold is caused by a contingency that includes the loss of the nuclear power plant and two 161 kV transmission components. The loss of these transmission components greatly reduces the flow of reactive power from resources located outside the problematic location.

The next step was is to find potential system upgrades that will lead to compliance with the transmission operator's transient voltage response requirements. Voltage profile problems are generally solved by system upgrades (addition of reactive power resources or transmission additions) that are electrically near the buses with the low voltage issues. Addition of reactive power resources is generally much more economical and also environmentally preferable to transmission additions. Thus dynamically controlled (static var compensator-SVC) reactive resources and fixed or mechanically switched capacitors banks were tried as potential solutions. Static voltage resources were already present in this location; however, the var capacity of the existing compensation was not large enough to improve the voltage dip and voltage recovery following fault clearing. Thus, additional static reactive compensation and a SVC were added. Transmission upgrades that the transmission operator had already planned to add in the near future were also incorporated. Then adjustments to the existing cap banks and SVC additions were performed until the transient voltage response requirement was met. The new reactive resources added to the grid in

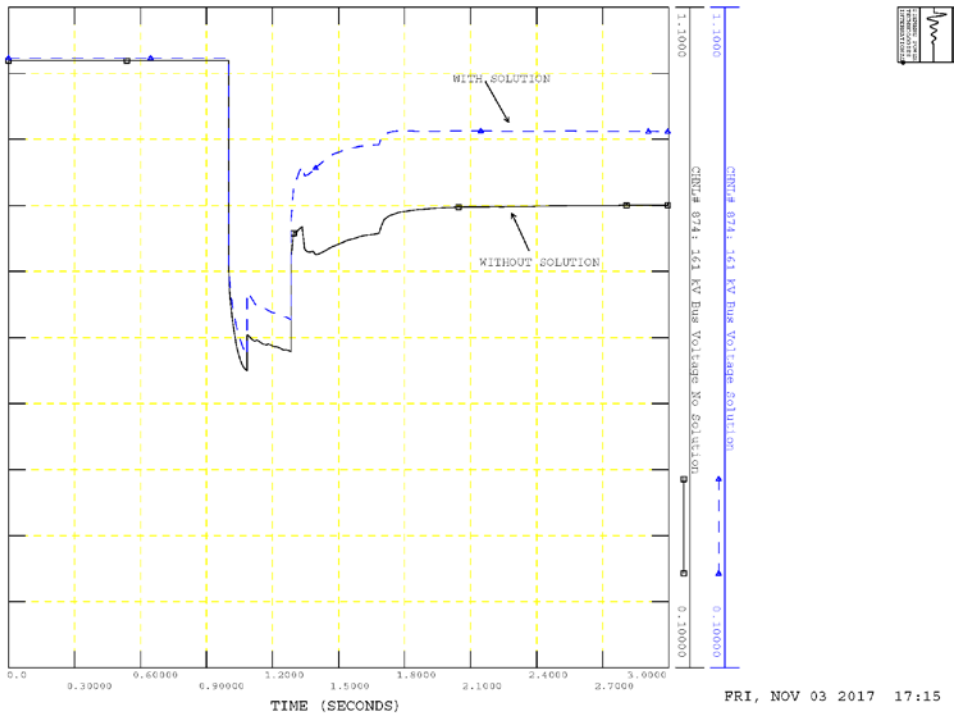

Figure 10. Plot of 161 kV bus voltage with (blue curve) and without (black curve) additional reactive resources and transmission upgrade

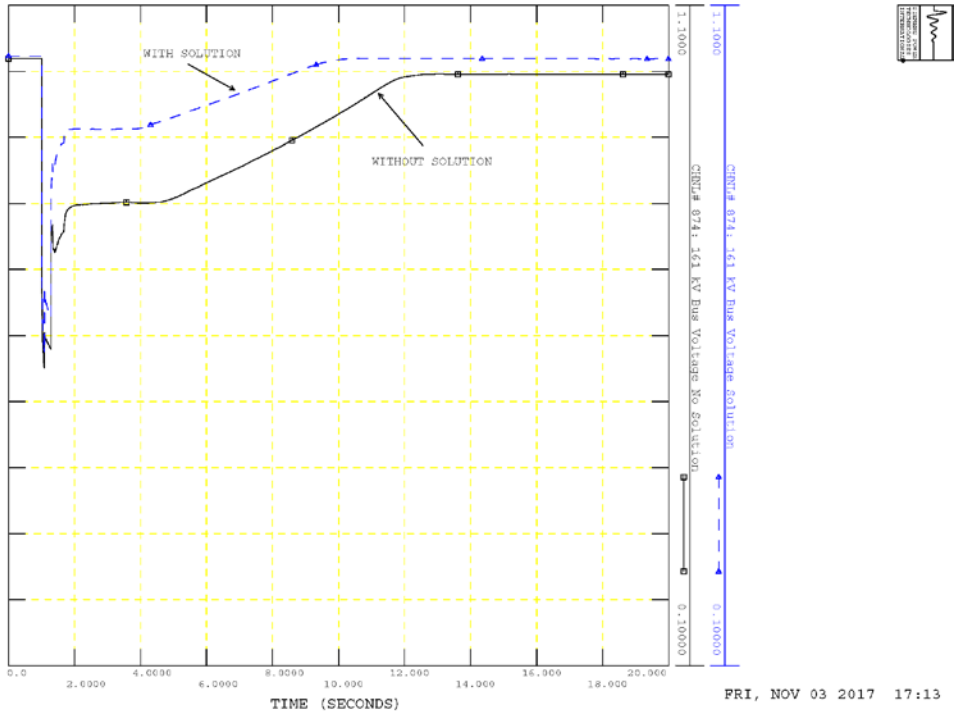

Figure 11. Plot of 161 kV bus voltage with (blue curve) and without (black curve) additional reactive resources and transmission upgrade (expanded time scale)

this critical location in the major load center amounts to about 30 Mvar of static reactive compensation and a total of 50 Mvar of dynamically controlled reactive compensation (SVC). These preliminary results are now undergoing refinement and may change. Figure 10 shows the critical bus voltage without any additional reactive resources (black curve) and with the additional reactive resources (blue curve). Without additional reactive resources the voltage does not recover adequately and fails the voltage recovery criteria, settling at about 0.8 pu. With the additional reactive resources described above, the voltage recovers and meets the voltage recovery criteria. Figure 11 shows the same two voltages with a longer time period of 20 seconds and the full recovery can be seen with the additional reactive resources.

6 Next Generation of Load Models

With the rapid increase in penetration of distributed energy resources (DER), transmission and distribution planners must adapt their study methodology and simulation models in order to account for this new type of equipments and its particular dynamics. In the past, net reduction of voltage dependent loads was the method most commonly used to account for energy resources at the sub-transmission and distribution levels. This approach is sufficient when the penetration level of DER into the distribution system is known to be low or not significant. However in many systems this practice is no longer sufficient moving forward, as the distribution system continues to have more DER integrated.

Load modeling working groups and similar task forces have been studying the most appropriate way to represent DER on distribution systems. This is an ongoing effort and the most accepted approach is the one proposed by NERC [14], in which various distributed generation models are plugged into the composite load model at the end of the distribution feeder model and/or at the low voltage side of the substation, as shown in Figure 12. The new composite load model proposition splits the DER into two different categories:

- Utility-Scale DER (U-DER)
  Representing relatively large solar PV power plants connected to the distribution or sub-transmission systems. These resources are generally 3-phase interconnections, and can range in capacity from 5 to 20 MW.

- Retail-Scale DER (R-DER)
  Representing resources that offset the customer load. These resources may include residential, commercial, and industrial customers. Typically, the residential units are single-phase while the commercial and industrial units can be single- or three-phase resources.

The U-DER model represents resources that have more complex controls associated with their interconnection. These resources could be modeled using detailed solar PV models, since the existing simulation models are capable of representing the dynamics of this DER resource with a comprehensive level of detail. The trade-off is the added complexity and set of data required for the detailed models, which can be burdensome. The U-DER model would allow the representation of these resources with a moderate degree of detail and complexity.

The R-DER model represents distributed generating resources throughout the distribution system whose controls are generally much less complex.

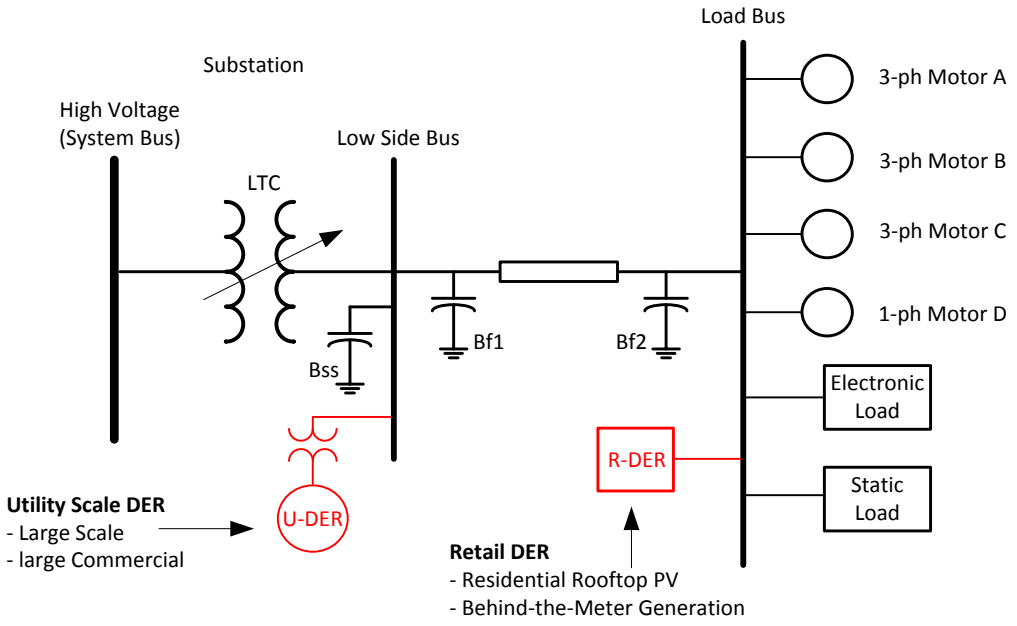

Figure 12. CLMD Including DER Representation

The recent developed PVD1 model (available in most software tools) is an attempt to represent U-DER and R-DER resources in a simplified, easy to use model. This model is a simple current injection with the capability to represent basic control strategies.

As mentioned previously, the development of models to represent DER in transient stability studies is still a work in progress and there are still limitations in the existing models related to their ability to represent some of the various functionalities that are being considered in the update of the California Rule 21 set of documents, as well as in the IEEE 1547 standard development, such as control of active and reactive power.

The newest proposed model to represent both U-DER and R-DER type of resources is called “DER_A”. This model is a simplified version of the existing utility-scale generic PV models with a notably reduced set of parameters. Despite the simplifications, this proposed model maintains several functional features which are in alignment with the IEEE 1547 standard and the California Rule 21 documents.

This model is currently undergoing final revisions. The available transient stability software tools have not yet made this model available for use, but the industry expectation is that these models will become available in the very near future.

7 Conclusions

It is important that the power system models include accurate representation of loads with respect to both voltage and time. When no information on the loads composition is available, algebraic equations are utilized to represent load variation with voltage. However, voltage dependent static load models work well only for system studies where the load composition does not have a high penetration of induction

motors, electronic loads, etc. In these situations, static load models are not sufficiently detailed, as they do not represent any load dynamics. Hence, system studies using traditional load modeling have not been able to replicate measured FIDVR. Load models that do not model all pertinent dynamics can result in studies that do not effectively identify potential FIDVR events.

The loads magnitude, composition and dynamics change with season, month, week, day and hour of the day. This seasonal and random nature of the loads makes its modeling difficult in power system studies. Detail load models representing its dynamics require a large amount of data that can turn the data gathering effort burdensome. There is an important trade-off to be taken into account between the effort of collecting data and the real need for detailed load representation in transient stability analysis.

The load modeling discussion and case study presented by this paper aids the electrical engineer in making decisions on when simplified load representations are enough to accomplish the objectives of the intended transient stability study or when detailed load representation is required to better identify potential FIDVR events and corresponding mitigation actions.

A comparison between simulation results and recorded system events is strongly recommended, in order to calibrate the detailed load models with regards to the amount of load lost (consequential and non-consequential), percentage of motors that stall, re-start, etc.

This importance of proper understanding of the load dynamics, its impacts in the system performance and consequently the need for adequate representation in system studies will continue to increase as system loads increase in complexity.

8 References

[1] "Definition and Classification of Power System Stability". IEEE/CIGRE Joint Task Force on Stability Terms and Definitions, IEEE Transactions on Power Systems, VOL. 19, NO. 2, May 2004, pp 1387-1401.

[2] "A Technical Reference Paper - Fault Induced Delayed Voltage Recovery", version 1.2, prepared by the North American Electric Reliability Corporation – Transmission Issues Subcommittee and System Protection and Control Subcommittee, dated June 2009.

[3] 2013 FIDVR Events Analysis on Valley Distribution Circuits. Richard Bravo and Steven Robles. December 30, 2013. (Available at https://certs.lbl.gov/sites/default/files/2013-fidvr-valley-distribution-circuits-events-analysis.pdf).

[4] "Final Project Report Load Modeling Transmission Research", prepared for CIEE by Lawrence Berkley National Laboratory, dated June 2010.

[5] Reactive Power Planning. NERC Reliability Guideline, December 2016. (Available at http://www.nerc.com/comm/PC_Reliability_Guidelines_DL/Reliability%20Guideline%20-%20Reactive%20Power%20Planning.pdf)

[6] NERC Standard PRC-024-2 - Generator Performance During Frequency and Voltage Excursions.

Reliability Standards for the Bulk Electric Systems of North America. (Available at www.nerc.com).

[7] PSS®E 34 - Program Operation Manual, Siemens Power Technologies International, March 2015

[8] Dynamic Load Modeling. NERC Technical Reference Document, December, 2016. (Available at http://www.nerc.com/comm/PC/LoadModelingTaskForceDL/Dynamic%20Load%20Modeling%20Tech%20Ref%202016-11-14%20-%20FINAL.PDF).

[9] Developing Load Model Composition Data. NERCD Reliability Guideline, Draft, March, 2017. (Available at http://www.nerc.com/pa/RAPA/rg/ReliabilityGuidelines/Reliability_Guideline_-_Load_Model_Composition_-_2017-02-28.pdf).

[10] MISO MOD-032 Model Data Requirements & Reporting Procedures, Version 1.1. July 15, 2016. (Available at https://www.misoenergy.org/Planning/Models/Pages/MOD-032.aspx).

[11] NERC Standard TPL-001-4 - Transmission System Planning Performance Requirements. Reliability Standards for the Bulk Electric Systems of North America. (Available at www.nerc.com).

[12] Latest Research on Load Modeling & Dynamic Behavior of Loads. Anish Gaikwad and Pouyan Pourbeik. Presented at the Panel Session: Advancements in Load Modeling for Dynamic Voltage Performance Analysis, IEEE PES General Meeting, July 20, 2016. (Available at http://resourcecenter.ieee-pes.org/product/-/download/partnumber/PESSLI1247).

[13] SCE FIDVR Study Experience. Jun Wen. Presented at the Panel Session: Advancements in Load Modeling for Dynamic Voltage Performance Analysis, IEEE PES General Meeting, July 20, 2016. (Available at http://resourcecenter.ieee-pes.org/product/-/download/partnumber/PESSLI1247).

[14] "Distributed Energy Resource Modeling". NERC Reliability Guideline, September 2017. (Available at http://www.nerc.com/pa/RAPA/rg/Pages/Reliability-Guidelines.aspx).

9 Biographies

Dr. Carlos Grande-Moran is an expert engineering professional with 40+ years of experience in analysis, development, design, functional specifications, documentation, planning, and operations problems related to electric power systems. He has worked extensively for world-renowned power systems manufacturing (GE - Power System Consulting Services and Generator Engineering, and Harris Corporation - Controls Division) and been involved in black start studies of large metropolitan and interconnected networks, torsional impact and subsynchronous resonance in industrial and large power systems, evaluation of frequency response, automatic underfrequency load shedding and automatic generation control dynamic impacts on system frequency, integration of renewable generation resources in conventional power systems, and the design and manufacture of large and medium size turbine-generators. This experience, when combined with his work for consulting service companies, electric utilities, as well as Universities in the United States and overseas, makes him uniquely suited to his position as Principal Consultant at Siemens PTI

 **Daniel. Feltes** has been involved in many power system reliability studies, performing steady state and dynamic analysis. His primary focus has been evaluating the impact of generation interconnections on the reliability of transmission networks. He has performed impact studies for both conventional and renewable sources of energy in several regions of the United States. He is proficient in PSS®E, PSS®MUST and Python® automation. He also has experience developing and testing dynamic simulation models

Dr. Ming Wu received the Bachelor degree and the Master degree of Engineering from Huazhong University of Science and Technology, China. He obtained the Ph.D. degree from Tulane University at New Orleans, Louisiana, USA. He owned a PE license from the State of Louisiana. Mr. Ming Wu worked as an application engineer at GE Energy Consulting in Schenectady, NY from 2001 to 2006. He joined METC and then ITC in Michigan in 2006 and has been working on power system time domain simulation since 2006

Robert Wells received his Bachelor of Science degree in Electrical Engineering from Iowa State University in December 2008. He joined ITC Midwest in January 2009 and is currently a Senior Engineer in the Transmission Planning department. Since 2009, he has worked in the Transmission Planning department and been involved in various planning functions, including generator interconnections, transmission service requests, load interconnections, 34.5 kV to 69 kV system conversion studies, black start system restoration plans, model building, annual system assessments (TPL), steady state studies, and dynamics studies.

 **Bernardo Fernandes** received his BSEE degree from State University of Rio de Janeiro (UERJ) in 1999 and his MSEE degree from Federal University of Rio de Janeiro (COPPE/UFRJ) in 2005. He joined Siemens PTI in 2007 and is currently the Head of the Power System Consulting Department. Most of his work at Siemens PTI has been in the area of transmission planning, generation interconnections of renewable energy and conventional plants, technical/economic evaluations, feasibility analyses, generator retirement studies and more. He is a Member of the IEEE and its Power Engineering Society.

 **James W. Feltes** received his BSEE degree with honors from Iowa State University in 1979 and his MSEE degree from Union College in 1990. He joined PTI, now Siemens PTI, in 1979 and is currently a Senior Manager in the Consulting Department. At PTI, he has participated in many studies involving planning, analysis and design of transmission and distribution systems. He is an instructor in several of the courses taught by PTI. He is a member of several IEEE committees, working groups, and task forces dealing with power system stability and control. He is a Senior Member of the IEEE and is a registered professional engineer in the state of New York.

Appendix A – Typical Parameters for the CMLD Model

CONs	Original No Trip Values	NERC Values	Values Used in Case Study	EPRI Trip Settings	WECC Trip Settings	Description
J	0	-1	0			Load MVA base
J+1	0	0	0			Substation shunt B (pu on Load MVA base)
J+2	0.01	0.04	0.01			Rfdr - Feeder R (pu on Load MVA base)
J+3	0.001	0.04	0.001			Xfdr - Feeder X (pu on Load MVA base)
J+4	0	0	0			Fb - Fraction of Feeder Compensation at substation end
J+5	0	0.08	0.06			Xxf - Transformer Reactance – pu on load MVA base
J+6	1	1	1			Tfixhs - High side fixed transformer tap
J+7	1	1	1			Tfixls - Low side fixed transformer tap
J+8	0	1	0			LTC - LTC flag (1 active, 0 inactive)
J+9	1	0.9	0.9			Tmin - LTC min tap (on low side)
J+10	1	1.1	1.1			Tmax - LTC max tap (on low side)
J+11	1	0.00625	0.0063			Step - LTC Tstep (on low side)
J+12	1	0.9875	0.98			Vmin - LTC Vmin tap (low side pu)
J+13	1	1.0125	1.02			Vmax - LTC Vmax tap (low side pu)
J+14	0	0.1	0.1			TD - LTC Control time delay (sec)
J+15	0	15	15			TC - LTC Tap adjustment time delay (sec)
J+16	0	0	0			Rcmp - LTC Rcomp (pu on load MVA base)
J+17	0	0	0			Xcmp - LTC Xcomp (pu on load MVA base)
J+18						FmA - Motor A Fraction
J+19						FmB - Motor B Fraction
J+20						FmC - Motor C Fraction
J+21						FmD - Motor D Fraction
J+22						Fel - Electronic Load Fraction
J+23	0.9	1	0.9			PFel - PF of Electronic Loads
J+24	0.6	0.7	0.6			Vd1 - Voltage at which elect. loads start to drop
J+25	0.4	0.5	0.4			Vd2 - Voltage at which all elect. load have dropped
J+26	0.95	-0.995	0.95			PFs - Static Load Power Factor
J+27	2	2	2			P1e - P1 exponent
J+28	0.615	0.5	0.615			P1c - P1 coefficient
J+29	1	1	1			P2e - P2 exponent
J+30	0.38	0.5	0.38			P2c - P2 coefficient
J+31	0	0	0			Pfrq - Frequency sensitivity
J+32	2	2	2			Q1e - Q1 exponent
J+33	-0.5	-0.5	-0.5			Q1c - Q1 coefficient
J+34	1	1	1			Q2e - Q2 exponent
J+35	1.5	1.5	1.5			Q2c - Q2 coefficient
J+36	0	-1	0			Qfrq - Frequency sensitivity
J+37	3	3	3			MtypA - Motor type
J+38	0.85	0.75	0.85			LFmA - Loading factor (MW/MVA rating)
J+39	0.04	0.04	0.04			RaA - Stator resistance
J+40	1.8	1.8	1.8			LsA - Synchronous reactance
J+41	0.12	0.12	0.12			LpA - Transient reactance
J+42	0.104	0.104	0.12			LppA - Sub-transient reactance
J+43	0.095	0.095	0.095			TpoA - Transient open circuit time constant
J+44	0.0021	0.0021	0			TppoA - Sub-transient open circuit time constant
J+45	0.1	0.1	0.1			HA - Inertia constant
J+46	0	0	0			etrqA - Torque speed exponent
J+47	0.6	0.7	0.65	0.65	0.6	Vtr1A - U/V Trip1 V (pu)
J+48	999	0.02	0.1	0.1	0.033	Ttr1A - U/V Trip1 Time (sec)
J+49	0.2	0.2	0.2	0.2	0.3	Ftr1A - U/V Trip1 fraction
J+50	999	1	0.1	0.1	1	Vrc1A - U/V Trip1 reclose V (pu)
J+51	999	999	999	9999	9999	Trc1A - U/V Trip1 reclose Time (sec)
J+52	0.4	0.5	0.5	0.5	0.5	Vtr2A - U/V Trip2 V (pu)
J+53	999	0.02	0.02	0.02	0.033	Ttr2A - U/V Trip2 Time (sec)
J+54	0.15	0.7	0.75	0.75	0.7	Ftr2A - U/V Trip2 fraction

CONs	Original No Trip Values	NERC Values	Values Used in Case Study	EPRI Trip Settings	WECC Trip Settings	Description
J+55	999	0.7	0.65	0.65	0.65	Vrc2A - U/V Trip2 reclose V (pu)
J+56	999	0.1	0.1	0.2	0.2	Trc2A - U/V Trip2 reclose Time (sec)
J+57	3	3	3			MtypB - Motor type
J+58	0.75	0.75	0.75			LFmB - Loading factor (MW/MVA rating)
J+59	0.03	0.03	0.03			RaB - Stator resistance
J+60	1.8	1.8	1.8			LsB - Synchronous reactance
J+61	0.19	0.19	0.19			LpB - Transient reactance
J+62	0.14	0.14	0.14			LppB - Sub-transient reactance
J+63	0.2	0.2	0.2			TpoB - Transient open circuit time constant
J+64	0.0026	0.0026	0.0026			TppoB - Sub-transient open circuit time constant
J+65	0.15	0.5	0.7			HB - Inertia constant
J+66	2	2	2			etrqB - Torque speed exponent
J+67	0.6	0.6	0.55	0.55	0.6	Vtr1B - U/V Trip1 V (pu)
J+68	999	0.02	0.02	0.02	0.033	Ttr1B - U/V Trip1 Time (sec)
J+69	0.15	0.2	0.3	0.3	0.35	Ftr1B - U/V Trip1 fraction
J+70	999	0.75	0.65	0.65	0.9	Vrc1B - U/V Trip1 reclose V (pu)
J+71	999	0.05	0.05	0.05	9999	Trc1B - U/V Trip1 reclose Time (sec)
J+72	0.4	0.5	0.55	0.5	0.5	Vtr2B - U/V Trip2 V (pu)
J+73	999	0.02	0.025	0.025	0.033	Ttr2B - U/V Trip2 Time (sec)
J+74	0.15	0.3	0.3	0.3	0.6	Ftr2B - U/V Trip2 fraction
J+75	999	0.65	0.6	0.6	0.85	Vrc2B - U/V Trip2 reclose V (pu)
J+76	999	0.05	0.05	0.05	0.2	Trc2B - U/V Trip2 reclose Time (sec)
J+77	3	3	3			MtypC - Motor type
J+78	0.75	0.75	0.75			LFmC - Loading factor (MW/MVA rating)
J+79	0.03	0.03	0.03			RaC - Stator resistance
J+80	1.8	1.8	1.8			LsC - Synchronous reactance
J+81	0.19	0.19	0.19			LpC - Transient reactance
J+82	0.14	0.14	0.14			LppC - Sub-transient reactance
J+83	0.2	0.2	0.2			TpoC - Transient open circuit time constant
J+84	0.0026	0.0026	0.0026			TppoC - Sub-transient open circuit time constant
J+85	0.15	0.1	0.5			HC - Inertia constant
J+86	2	2	2			etrqC - Torque speed exponent
J+87	0.6	0.65	0.58	0.58	0.6	Vtr1C - U/V Trip1 V (pu)
J+88	999	0.02	0.03	0.03	0.033	Ttr1C - U/V Trip1 Time (sec)
J+89	0.15	0.2	0.2	0.2	0.35	Ftr1C - U/V Trip1 fraction
J+90	999	1	0.68	0.68	0.9	Vrc1C - U/V Trip1 reclose V (pu)
J+91	999	9999	0.05	0.05	9999	Trc1C - U/V Trip1 reclose Time (sec)
J+92	0.4	0.5	0.53	0.53	0.5	Vtr2C - U/V Trip2 V (pu)
J+93	999	0.02	0.03	0.03	0.033	Ttr2C - U/V Trip2 Time (sec)
J+94	0.15	0.3	0.3	0.3	0.6	Ftr2C - U/V Trip2 fraction
J+95	999	0.65	0.62	0.62	0.85	Vrc2C - U/V Trip2 reclose V (pu)
J+96	999	0.1	0.05	0.05	0.2	Trc2C - U/V Trip2 reclose Time (sec)
J+97	0.033	0.03	0.033		0.03	Tstall - stall delay (sec)
J+98	0.4	0.3	0.4		0.3	Trestart - restart delay (sec)
J+99	0.02	0.025	0.02		0.025	Tv - voltage input time constant (sec)
J+100	0.02	0.025	0.02			Tf - frequency input time constant (sec)
J+101	1	1	1		1	CompLF - compressor load factor, p.u. of rated power
J+102	0.97	0.98	0.97		0.98	CompPF - compressor power factor at 1.0 p.u. voltage
J+103	0.6	0.6	0.6		0.56	Vstall - compressor stall voltage at base condition (p.u.)
J+104	0.124	0.1	0.124		0.1	Rstall - compressor motor res. with 1.0 p.u. current
J+105	0.1	0.1	0.1		0.1	Xstall - compressor motor stall reactance - unsat.
J+106	0	0	0			LFadj - Load factor adjustment to the stall voltage
J+107	0	0	0			Kp1 - real power constant for running state 1
J+108	1	1	1			Np1 - real power exponent for running state 1
J+109	6	6	6			Kq1 - reactive power constant for running state 1

CONs	Original No Trip Values	NERC Values	Values Used in Case Study	EPRI Trip Settings	WECC Trip Settings	Description
J+110	2	2	2			Nq1 - reactive power exponent for running state 1
J+111	12	12	12			Kp2 - real power constant for running state 2
J+112	3.2	3.2	3.2			Np2 - real power exponent for running state 2
J+113	11	11	11			Kq2 - reactive power constant for running state 2
J+114	2.5	2.5	2.5			Nq2 - reactive power exponent for running state 2
J+115	0.86	0.86	0.86			Vbrk - compressor motor "breakdown" voltage (p.u.)
J+116	0.2	0.2	0.2			Frst - fraction of motors capable of restart
J+117	0.6	0.95	0.6		0.95	Vrst - voltage at which motors can restart (p.u.)
J+118	1	1	1			CmpKpf - real power constant for freq dependency
J+119	-3.3	-3.3	-3.3			CmpKqf - reactive power constnt for freq dependency
J+120	0.5	0.5	0.5		0.5	Vc1of f - Voltage 1 at which contactors start dropping out (p.u.)
J+121	0.4	0.4	0.4		0.4	Vc2off - Voltage 2 at which all contactors drop out (p.u.)
J+122	0.6	0.6	0.6		0.6	Vc1on - Voltage 1 at which all contactors reclose (p.u.)
J+123	0.5	0.5	0.5		0.5	Vc2on - Voltage 2 at which contactors start reclosing (p.u.)
J+124	10	15	15		15	Tth - compressor motor heating time constant(sec)
J+125	999	0.7	0.7		0.7	Th1t - temp at which comp. motor begin tripping
J+126	999	1.9	1.9		1.9	Th2t - temp at which comp. all motors are tripped
J+127	0	0.1	0.1		0.1	Fuvr - fraction of comp. motors with U/V relays
J+128	0	0.6	0.6		0.6	UVtr1 - 1st voltage pick-up (p.u.)
J+129	0.2	0.02	0.02		0.02	Ttr1 - 1st definite time voltage pickup (sec)
J+130	0	1	0		1	UVtr2 - 2nd voltage pick-up (p.u.)
J+131	5	9999	9999		9999	Ttr2 - 2nd definite time voltage pickup (sec)
J+132	N/A	0.8	0.8			Fraction of electronic load that can restart